Molecular Microbiology (2008) 68(5), 1196–1215 ■
doi:10.1111/j.1365-2958.2008.06221.x
First published online 9 April 2008

Hysteretic and graded responses in bacterial two-component signal transduction

Oleg A. Igoshin,[1]* Rui Alves[2] and Michael A. Savageau[3]
[1]*Department of Bioengineering, Rice University, Houston, TX 77251-1892, USA.*
[2]*Departament de Ciencies Mediques Basiques, Universidad de Lleida and IRB Lleida, Lleida, Spain.*
[3]*Department of Bioengineering, University of California – Davis, Davis, CA 95616, USA.*

Summary

Bacterial two-component systems (TCS) are key signal transduction networks regulating global responses to environmental change. Environmental signals may modulate the phosphorylation state of sensor kinases (SK). The phosphorylated SK transfers the phosphate to its cognate response regulator (RR), which causes physiological response to the signal. Frequently, the SK is bifunctional and, when unphosphorylated, it is also capable of dephosphorylating the RR. The phosphatase activity may also be modulated by environmental signals. Using the EnvZ/OmpR system as an example, we constructed mathematical models to examine the steady-state and kinetic properties of the network. Mathematical modelling reveals that the TCS can show bistable behaviour for a given range of parameter values if unphosphorylated SK and RR form a dead-end complex that prevents SK autophosphorylation. Additionally, for bistability to exist the major dephosphorylation flux of the RR must not depend on the unphosphorylated SK. Structural modelling and published affinity studies suggest that the unphosphorylated SK EnvZ and the RR OmpR form a dead-end complex. However, bistability is not possible because the dephosphorylation of OmpR~P is mainly done by unphosphorylated EnvZ. The implications of this potential bistability in the design of the EnvZ/OmpR network and other TCS are discussed.

Accepted 14 March, 2008. *For correspondence. E-mail igoshin@rice.edu; Tel. (+1) 713 348 5502; Fax (+1) 713 348 5877.

Introduction

Cells respond to environmental signals via signal transduction pathways. Chief among these pathways is the class of phosphorylation cascades (Beier and Gross, 2006; Calva and Oropeza, 2006; Mascher, 2006; Mascher *et al.*, 2006). In a phosphorylation cascade, the first protein responds to a signal, and changes the phosphorylation levels of some other downstream protein. These phosphorylation changes continue until they modulate the activity of a final set of protein targets, which then modulate protein activity and/or gene expression.

Bacteria use a special type of phosphorylation cascade known as two-component systems (TCS) (see Stock *et al.*, 2000; Mizuno, 2005; Mascher *et al.*, 2006 for reviews). The basic motif (Fig. 1A) of the TCS is a sensor kinase (SK) protein (sometimes also called histidine kinase) that changes its phosphorylation state in response to a signal and that once phosphorylated transfers its phosphate to a response regulator (RR) protein. This is the prototype of a classical TCS. Phosphorylated RR will then cause a physiological response in the cell. Variations on this motif include phosphorelays (Hoch and Varughese, 2001; Stephenson and Hoch, 2002) in which three or four steps of phosphotransfer occur before the final modulator of cellular activity is activated.

In many cases (Stock *et al.*, 2000) the SK has another function: when it is unphosphorylated, it dephosphorylates its cognate RR (Fig. 1A). The phosphatase activity of the SK can often serve as an alternative or additional sensor of the environmental signals (Jin and Inouye, 1993; Pioszak and Ninfa, 2003). What is the role of such a bifunctional design? Previously, we have analysed the physiological consequences of variations in the design of TCS (Alves and Savageau, 2003). It was found that a classical TCS in which the sensor is bifunctional (that is, the phosphorylated sensor phosphorylates the RR and the unphosphorylated sensor enhances dephosphorylation of the RR) is more efficient in amplifying the signal and in buffering against cross talk than a TCS with a monofunctional sensor (without the SK phosphatase activity towards RR~P). On the other hand, the TCS with a monofunctional sensor is more effective in integrating signals from different sources. Other researchers have suggested additional roles for bifunctionality: mathemati-

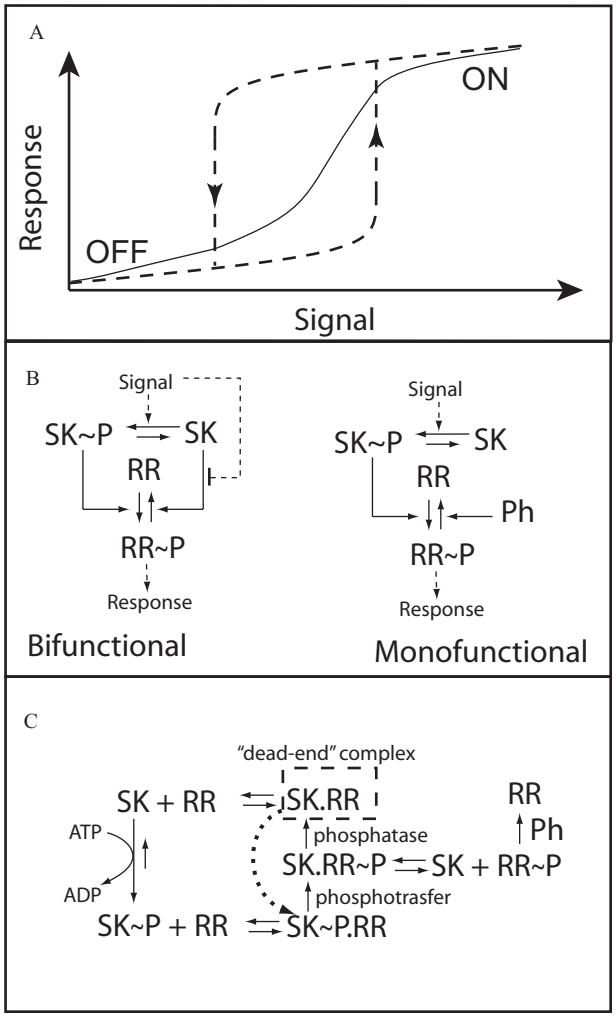

Fig. 1. A. Alternative network designs for classical TCS modules. B. SK denotes the unphosphorylated sensor kinase, and RR the unphosphorylated response regulator; phosphorylated forms of these proteins are denoted as SK~P and RR~P, respectively. The left-hand side of the panel represents a monofunctional design, in which SK~P phosphorylates the RR and the dephosphorylation of the RR~P is catalysed by an alternative phosphatase. The right-hand side of the panel represents a bifunctional design, in which the SK~P phosphorylates the RR and the SK dephosphorylates the RR~P. Schematic representation of graded (monostable, solid line) and hysteretic (bistable, dashed line) responses.
C. Reaction scheme for a generic two-component system. For simplicity, the release of inorganic phosphate is not depicted and the mechanistic details of the alternative phosphatase (Ph) reactions are omitted. See Table 1 for details on how the use of different values for the parameters of this scheme allows us to model the alternative designs shown in (A). Period (.) denotes protein binding complex.

cal models suggest that the systemic response of the TCS module will be insensitive to variations of protein concentration (Russo and Silhavy, 1991; 1993; Batchelor and Goulian, 2003).

The response to external signals can exhibit qualitatively different shapes. The cell can respond to changes in an external signal in a graded (continuous) way (Fig. 1B). Many examples exist with this type of response. However, recently there has been a surge of interest in an alternative type of response that leads to discontinuous, switch-like behaviour. Some signal transduction pathways will respond gradually only up to a certain threshold level of the increasing signal. Changes in the input signal above that threshold will shift the steady-state concentrations of the proteins to a new level in a discontinuous manner. When the intensity of the signal decreases, the state of the signal transduction pathway will decrease accordingly down to a lower threshold level of phosphorylation (Fig. 1A). Below this level, the system discontinuously jumps to its low signal state. The system can reach two stable steady states if signal intensities lies between the two thresholds for the discontinuous jumps, i.e. for certain parameter values the system is bistable. The steady-state output of the system will depend upon its initial state when the signal is received. Because of this, the response is termed hysteretic.

The classic and most noted example of bistability is induction of the lactose operon with gratuitous inducers (Novick and Weiner, 1957; Monod and Jacob, 1961). The critical conditions for this phenomenon could not have been known at the time, and it has been widely interpreted in the literature that the *lac* operon responds in the all-or-none fashion to the substrate lactose. It was subsequently discovered that the natural inducer of the lactose operon is allolactose (Jobe and Bourgeois, 1972), and that the inducible β-galactosidase enzyme not only catalyses the synthesis of allolactose but also its conversion to the products galactose and glucose (Huber *et al.*, 1975). This additional mechanistic information allowed for the derivation of a simple condition for hysteresis (Savageau, 1999). In addition to cooperativity expressed at the level of transcription initiation, the condition involves a critical relationship between the kinetic orders (with respect to the inducible enzymes and transporters) of the aggregate production and elimination of inducer. This condition gives an explanation for the classical experiment of Novick and Weiner (1957) and that of Sadler and Novick (1965), which provided an experimental demonstration of the cooperativity. Moreover, this condition shows why induction with the substrate lactose is not expected to be an all-or-none hysteretic response (Savageau, 2001). As far as we are aware there is no experimental evidence for such a response, even when it has been specifically looked for with modern experimental techniques (Ozbudak *et al.*, 2002).

Bistability has been observed in several other biological systems (see for example Ferrell, 2002; Dubnau and Losick, 2006 for reviews) and the mechanistic requirements for the existence of bistability in biological networks have been theoretically analysed (Thomas and Richelle,

1988; Savageau, 2001; Angeli *et al.*, 2004; Craciun *et al.*, 2006) Examples of natural bistability in bacteria include the decision between lysis and lysogeny fates of phage lambda in *Escherichia coli* (Ptashne, 2004) and expression of late stationary phase genes in *B. subtilis* (Maamar and Dubnau, 2005; Veening *et al.*, 2005; 2008; Suel *et al.*, 2006; Maamar *et al.*, 2007). Many more examples of bistability have been observed in artificial constructs, particularly as a result of theory-guided synthetic biology approaches (for instance Gardner *et al.*, 2000; Tchuraev *et al.*, 2000; Becskei *et al.*, 2001; Atkinson *et al.*, 2003; Isaacs *et al.*, 2003; Kobayashi *et al.*, 2004; Kramer and Fussenegger, 2005; Ajo-Franklin *et al.*, 2007). All the systems mentioned above display bistability because of positive feedback loops that include transcription and translation. However, bistability-enabling positive feedback loops can also originate at the post-translational level as in the partner-switching network controlling activity of the sporulation-controlled sigma factor σ^F (Igoshin *et al.*, 2006). A similar post-transcriptional feedback mechanism has also been predicted in eukaryotic MAP kinase cascade (Markevich *et al.*, 2004). Such post-transcriptional feedback loops facilitate fast activation of transcription factors on a faster biochemical time scale because no new protein synthesis is required.

In this work we analyse further implications of bifunctionality in shaping the TCS response. We ask if and under which conditions hysteric bistability can be found in bacterial TCS signal transduction. To address the bistability question we analyse and compare the systemic behaviour of models of classical TCS with monofunctional SK to that of models of classical TCS with bifunctional SK. Our goals in doing this are threefold. First, we aim to elucidate the conditions for a bistable response in generic TCS without transcriptional feedbacks, underlining the key interactions required for this bistability. Second, we qualitatively analyse specific experimental examples of TCS and predict whether bistability is possible or not in those TCS, while interpreting the results within the physiological context of the experimental systems. Third, we choose the EnvZ/OmpR system to perform a quantitative analysis of a kinetically well-characterized TCS. This system was chosen because (i) it is a classic prototypical TCS that does not require auxiliary proteins for its core function; (ii) it is well characterized in terms of kinetic parameters; (iii) both the dimerization domain of the SK and the receiver domain of the RR have been partially crystallized; and (iv) it has been reported to respond in a graded fashion. Alternative choices, with well-characterized kinetic parameters and partially crystallized and resolved structures that might be considered include the CheA system (Baker *et al.*, 2006), the Spo system (Stephenson and Hoch, 2002; Piggot and Hilbert, 2004) and the Ntr system (Jiang *et al.*, 2000a,b; Pioszak and Ninfa, 2003). However, these systems are less appropriate for our general analysis. For instance, the Spo and Ntr system are not the classical prototype of a TCS. The Ntr system includes an additional protein that modulates the kinetic activity of NtrB, thus being a 'three-component system'. The Spo system is in reality a four-step phosphorelay. Although we have not focused on these more complex TCS, we will address the applicability of our results to these and other systems in the *Discussion* section.

By using the EnvZ/OmpR TCS we can identify, for the simplest prototype TCS with a graded response, specific features that are to be changed if the system is to have a bistable switch-like response. Pinpointing the origin of bistability for TCS may have important consequences for our understanding of different aspect of bacterial behaviour, such as (i) bacterial differentiation, (ii) lifestyle switches during pathogenesis, or (iii) bacterial strains with synthetic signal transduction modules designed to create specific biotechnological behaviour. The results of this analysis for the EnvZ system should be relevant to other systems, as available data suggest that parameters for equivalent reactions are similar among different TCS (see *Discussion* and references therein).

Results

Brief discussion of the model and our assumptions

In this section we briefly describe the generic model for the TCS used in our simulations and how we refined this model using the EnvZ/OmpR system as an example. The details of the model reactions, assumptions and parameters are given in the *Experimental procedures* section. Below we briefly review the key features of the model (Fig. 1B and C). The model is based on a modified version of the kinetic scheme proposed by Batchelor and Goulian (2003). However, several reactions and states are included in our model, in addition to those proposed by Batchelor and Goulian.

Additional reactions include autodephosphorylation of the RR and dephosphorylation of the RR by an alternative phosphatase (Ph) (Perego *et al.*, 1996; Perego and Hoch, 1996; Mizuno, 1998; Parkinson, 2003). Although the later is not observed in the EnvZ/OmpR system, it will allow us to compare the behaviour of the system to that of an equivalent monofunctional TCS by adjusting kinetic parameters; this is relevant because several monofunctional TCS include such Ph (Perego *et al.*, 1996; Perego and Hoch, 1996).

To set up the model we surveyed available experimental data for the EnvZ/OmpR system – one of the most well-studied TCS in the literature. Various biochemical assays *in vitro* (Qin *et al.*, 2001; Cai and Inouye, 2002;

Table 1. Reactions and parameter values used for numerical simulations.

Reaction numbers and types		Parameters and values	
No.	Type	Bifunctional design	Monofunctional design
1	SK → SK~*P* + ADP – ATP	k_{ap}, variable k_{ap} = 0.1 s^{-1} (Fig. 2B, Figs S1, S2 and S4B)	k_{ap}, variable
2	SK~P → SK + P_i	k_{ad} < 0.001 s^{-1}	k_{ad} = 0.001 s^{-1}
3	SK~*P* + RR → SK~P.RR	k_{b1} = 0.5 μM s^{-1}	k_{b1} = 0.5 μM s^{-1}
4	SK~P.RR → SK~*P* + RR	k_{d1} = 0.5 s^{-1}	k_{d1} = 0.5 s^{-1}
5	SK~P.RR → SK.RR~P	k_{pt} = 1.5 s^{-1}	k_{pt} = 1.5 s^{-1}
6	SK.RR~P → SK + RR~P	k_{d2} = 0.5 s^{-1}	k_{d2} = 0.5 s^{-1}
7	SK + RR~P → SK.RR~P	k_{b2} = 0.5 μM s^{-1} k_{b2} = 0.05 μM s^{-1} (Fig. 2B and C, Figs S1, S2 and S4B)	k_{b2} = 0.05 μM s^{-1}
8	SK.RR~P → SK.RR + P_i	k_{ph} = 0.05 s^{-1} k_{ph} = 0.025 s^{-1} (Fig. S3, grey thick line)	k_{ph} = 0 s^{-1}
9	SK.RR → SK + RR	k_{d3} = 0.5 s^{-1}	k_{d3} = 0.5 s^{-1} k_{d3} = 5 s^{-1} (Figs 2A and A3, dash-dotted line)
10	SK + RR → SK.RR	k_{b3} = 0.5 μM s^{-1}	k_{b3} = 0.5 μM s^{-1}
11	Ph + RR~P → Ph.RR~P	k_{b4} = 0.5 μM s^{-1} (Fig. 2B, Figs S1, S2 and S4B)	k_{b4} = 0.5 μM s^{-1}
12	Ph.RR~P → Ph + RR~P	k_{d4} = 0.5 s^{-1}(Fig. 2B and C, Figs S1, S2 and S4B)	k_{d4} = 0.5 s^{-1}
13	Ph.RR~P → Ph + RR	k_{cat} = 0.025 s^{-1} (Fig. 2B and C, Figs S1, S2 and S4B)	k_{cat} = 0.05 s^{-1} k_{cat} = 0.1 s^{-1} (Fig. S3, dash-dotted line)
		$[RR]_{total}$ = 6 μM $[SK]_{total}$ = 0.17 μM $[Ph]_{total}$ = 0 $[Ph]_{total}$ = 0.17 μM (Fig. 2B and C, Figs S1, S2 and S4B)	$[RR]_{total}$ = 6 μM $[SK]_{total}$ = 0.17 μM $[Ph]_{total}$ = 0.17 μM

Yoshida *et al.*, 2002a,b) allowed us to estimate the values for the network parameters. The details are given in the *Experimental procedures* section and summarized in Table 1. We note that different research groups have expressed alternative views on the role of EnvZ in the dephosphorylation of OmpR. Mattison and Kenney (2002) found evidence for low affinity of phosphorylated OmpR with EnvZ and raised doubts about the importance of EnvZ in the dephosphorylation of OmpR *in vivo* (monofunctional design). On the other hand, subsequent findings by Yoshida *et al.* (2002a) questioned these conclusions and presented evidence that both phosphorylated and unphosphorylated forms of the OmpR interact with EnvZ with similar affinities. These data and previous findings support the idea of an essential role for EnvZ in OmpR dephosphorylation (bifunctional design). The scheme presented in Fig. 1C allows either bifunctional or monofunctional designs to be modelled by adjusting the rates of protein binding and of the dephosphorylation reactions. In subsequent sections we compare the transient and steady-state performance of both designs.

The experimental evidence suggesting that the affinity of the RR for phosphorylated or unphosphorylated SK is not very different (Yoshida *et al.*, 2002a) prompted us to include a reversible reaction in which the unphosphorylated forms of RR and SK can form a complex (SK.RR). Such a complex can also result from the phosphatase action of unphosphorylated EnvZ upon the phosphorylated RR. What is the fate of the SK.RR complex? Two alternatives exist: (i) The SK in the complex can still autophosphorylate and subsequently transfer its phosphate to the RR (reaction shown by the dashed line in Fig. 1C) or (ii) binding of the RR interferes with *trans*-autophosphorylation of EnvZ by its dimer partner and therefore dissociation of the RR is required for subsequent EnvZ autophosphorylation. Because we could find no data in the literature to support one view or the other, we used structural bioinformatics to further analyse this issue. Our analysis (Appendix A) of the structure of the complex between EnvZ dimer and OmpR indicates that binding of OmpR to one of EnvZ subunit is likely to disturb access of the His243 residue of this subunit to the ATP-binding domain of another EnvZ subunit, thus preventing *trans*-phosphorylation of this residue. Therefore, the SK.RR complex would be a 'dead-end' – its dissociation would be required for SK to autophosphorylate. Thus, we excluded the possibility of autophosphorylation for the SK while in the SK.RR complex and we eliminated this reaction (dashed arrow on Fig. 1C) from the model.

Steady-state responses in bifunctional and monofunctional systems

The balance between the phosphatase and kinase activity is affected by the phosphorylation state of EnvZ. Therefore, the rate of EnvZ autophosphorylation can serve as one important physiological input of the system to determine this balance. Another important physiological input may be modulation of the SK phosphatase activity (Jin and Inouye, 1993; Pioszak and Ninfa, 2003). The concen-

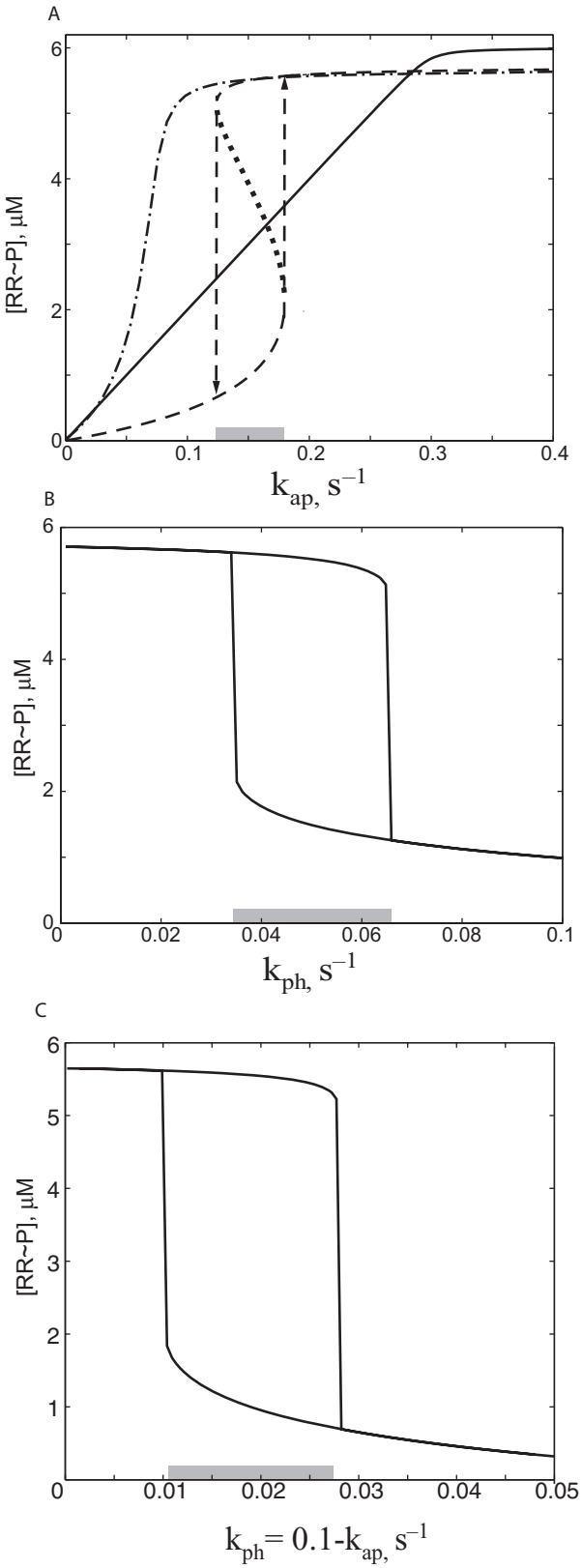

Fig. 2. Steady-state response as a function of (A) the autophosphorylation rate of the sensor kinase; (B) the phosphatase rate of the bifunctional SK and (C) changes in both rates.
A. The bifunctional TCS (solid line) shows a linear increase in the concentration of phosphorylated RR ([RR~P]) until the pool of the RR is 100% phosphorylated. The monofunctional system with an alternative phosphatase dephosphorylating RR~P shows a bistable response (dashed lines). The system jumps from one steady state to another (arrows) at threshold values of the autophosphorylation rate. The unstable steady states are shown by a dotted line. Shaded region indicates values of rate constants for which system is bistable. Bistability depends on the long lifetime of the dead-end complex between unphosphorylated RR and SK; a 10-fold decrease in their affinity results in a graded response (dash-dotted line).
B. Bistability of the bifunctional TCS in the presence of an alternative phosphatase. The steady-state concentration of RR~P decreases with an increasing rate of the bifunctional SK phosphatase while autophosphorylation rate is kept constant. In the intermediate range of phosphatase rates (shaded region) the system is bistable, jumping from one steady state to another at the boundaries.
C. Same as (B) but with the autophosphorylation rate linearly decreasing with increasing phosphatase rate as indicated on axis label.

tration of phosphorylated RR OmpR is the physiologically relevant output of the model because binding of this form to multiple promoters determines the level of gene expression of OmpC, OmpF and several other genes.

In Fig. 2A we plot the steady-state level of phosphorylated RR as a function of the autophosphorylation rate of SK for a fixed phosphatase activity of SK. The concentration of RR~P increases linearly with the autophosphorylation rate of SK for the bifunctional design, before saturating with 100% of the RR phosphorylated. These results concur with predictions by Batchelor and Goulian (2003). In both models, the slope of the curve that plots RR phosphorylation levels as a function of SK autophosphorylation rate is independent of SK concentration. Furthermore, in our model, this slope is not sensitive to the formation of the SK.RR dead-end complex.

The monofunctional design behaves differently from the bifunctional design, with the monofunctional circuit working as a switch and displaying hysteretic bistability: two stable steady states (dashed lines in Fig. 2A) exist for an intermediate range of autophosphorylation rates (depicted by the shaded bar in Fig. 2A). Depending on the initial conditions (initially ON or initially OFF), the system can reach either of two steady states. The steady-state concentration of RR~P discontinuously jumps from one branch to another at the boundaries of the bistable region as indicated by the arrows at the threshold values of the autophosphorylation rate denoted as ON and OFF thresholds. For values below the OFF threshold, only the OFF state exists; for values above the ON threshold only the ON state exists. For values between the thresholds, the system is bistable and two stable steady states are separated by an unstable one (dotted line in Fig. 2A).

Stochastic fluctuations over the unstable state will lead to spontaneous switching.

A few factors are important for the observed bistability in the monofunctional design. The formation of an SK.RR (EnvZ.OmpR) dead-end complex, its long lifetime, and the absence of bifuctionality are key for the existence of bistability in the system. Indeed, when the affinity between unphosphorylated SK and RR is decreased 10-fold (Fig. 2A, dash-dotted line) no bistability is observed. Similar results are obtained if the SK.RR complex is not 'dead-end', i.e. RR binding does not interfere with autophosphorylation of SK. See the *Discussion* for an intuitive explanation of why this is so.

Can bistability be observed for a bifunctional TCS that responds to the environmental cues by changing the phosphatase activity of the SK protein (with a constant autophosphorylation rate)? Simulations shown on Fig. 2B demonstrate that, in the presence of an alternative phosphatase activity that constitutively dephosphorylates RR~P, the system displays hysteretic bistability. This bistability is observed over the intermediate range of SK phosphatase rates. Bistability can also be observed if the RR has constitutive autophosphotase activity. However, if this is the case, bistability is observed over a smaller range of parameter values (data not shown). To summarize, our results emphasize one fact. The existence of a major flux channel for the dephosphorylation of the RR~P that is independent of the unphosphorylated SK is the critical factor for a TCS to have a bistable response. Whether a SK is monofunctional or bifunctional is not a determinant for bistability.

The bistability range is further enhanced in the case when both autophosphorylation rate and phosphatase rate are affected by the signal (Fig. 2C). In several natural TCS the balance of kinase and phosphatase activity of SK depends on its conformation (Jin and Inouye, 1993; Zhu *et al*., 2000; Pioszak and Ninfa, 2003). If one assumes that each unphosphorylated SK can be in two conformational forms (one form with large phosphatase activity and another form with large autophosphorylation activity), then there is a negative linear relationship between kinase and phosphatase rate constants (see *Modeling procedures*). Under such conditions, the system displays bistability, with the OFF signal threshold being about three times higher than the ON signal threshold (Fig. 2C).

Range of parameter values that supports bistability

The parameter values chosen for our simulations are estimated from *in vitro* measurements for the EnvZ/OmpR system (Table 1 and *Modeling procedures*). However, to investigate the applicability of our conclusions to an *in vivo* situation, and to other TCS, we analysed the robustness of the bistability predictions against variations in parameter values. Because the parameter space is multidimentional, it cannot be easily represented graphically. Therefore, we opted to vary the parameter values in pairs and show how the range of input signals that supports bistability changes with the other model parameters (see *Modeling procedures* for technical details).

The results shown of Fig. 3 are for the bistable monofunctional TCS that responds to environmental clues through modulation of its autophosphorylation rate (as in Fig. 2A). The nine panels correspond to nine relevant parameters (see *Modeling procedures* for definitions) that determine the steady state of the system. Variation in the values for some of the parameters – an increase in total RR concentration or a decrease in the value of the binding constant for the formation of the dead-end complex – will increase the range of the bistability. Variation in the values for other parameters may lead to shrinkage and eventual disappearance of the bistable region. However, the overall results demonstrate that bistability is observed over at least a several-fold variation in the values of these parameters.

Similar results can be obtained for the bistable bifunctional TCS with an additional Ph that responds to environmental clues through modulation of its phosphatase rate (as in Fig. 2B). Bistability in this system is less robust than that in the monofunctional system, with respect to some parameters (Fig. S1). However, bistability becomes more robust with an increase of the phosphotransfer rate (Fig. S2). It should be noted that, for some parameter values, a low RR~P state is stable for all values of the phosphatase rate and that no transition from the low RR~P to the high RR~P state can occur, regardless of the value for the SK phosphatase activity. For these parameter values, an additional or alternative input to the system is required for transitions to occur between steady states.

Time and frequency responses of bistable and monostable designs

Several methodologies were used to quantitatively characterize the temporal responsiveness of the TCS because the transient response depends dramatically on the shape and amplitude of the input signal. In our first set of simulations (Fig. 4A and B), we investigated the responsiveness of two alternative TCS designs to an instantaneous change in the autophosphorylation rate. The dynamics of the approach to a new steady state is computed for both designs[1]: the top panel corresponds to the monofunctional, bistable system and the bottom panel to the bifunctional, monostable system. The numbers on the lines are com-

[1]Hereafter we refer to two aspects of design. One is the network aspect, which can be either bifunctional of monofunctional, the other is the dynamic aspect, which can be either bistable (hysteretic) or monostable (graded).

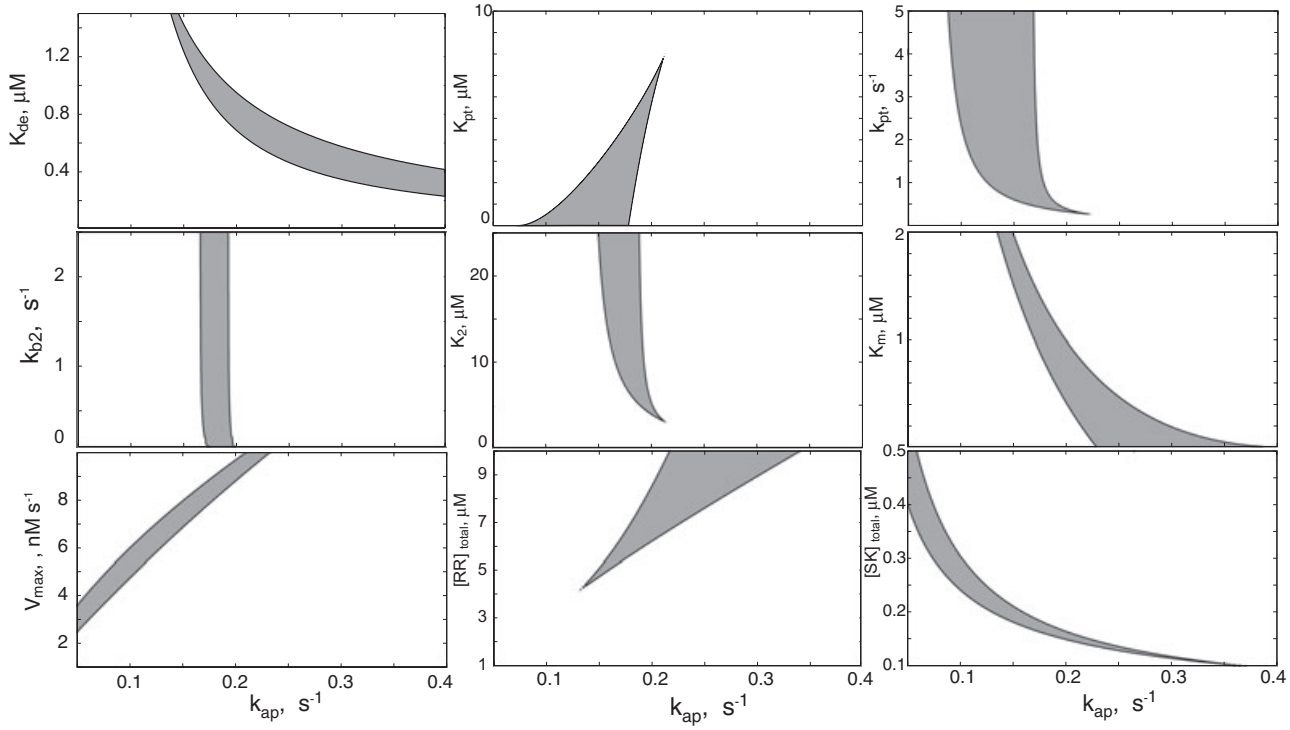

Fig. 3. Robustness of bistability in monofunctional TCS. Each panel is a two-dimensional section of the parameter space in which bistability is manifested. In each case, the *x*-axis represents values for the autophosphorylation rate k_{ph} and the *y*-axis represents values for one of the other parameters in the model; each physically realizable region of bistability is shaded in grey for each two-dimensional section of parameter space. In each panel, the parameters not explicitly represented are held constant at their values used in Fig. 2 (and summarized in Table 1). The definitions of the parameters are given in Table 1 and in the *Modeling procedures* section: K_{de} – dissociation constant of the SK.RR dead-end complex, k_{pt} – Michaelis–Menten constant of the phosphotransfer reaction, k_{pt} – rate constant for the molecular activity of the phosphotransfer reaction, K_2 – dissociation constant of the SK–RR~P complex, k_{b2} – rate constant for the binding of SK to RR~P, K_m – Michaelis–Menten constant of the phosphatase reaction, V_{max} – maximal velocity of the phosphatase reaction, $[SK]_{total}$ – total concentrations of SK, and $[RR]_{total}$ – total concentrations of RR.

puted response times defined as the time at which 90% of the full-scale response is achieved. Figure 4A depicts the response to an instantaneous increase in autophosphorylation rate: the system is initially in the steady state corresponding to $k_{ap} = 0.05\ s^{-1}$, defined as the starting state. This state is below the switching thresholds (here and below these are the thresholds defined for the bistable design in Fig. 2); the precise value of the rate for the starting state does not affect our conclusions (data not shown). At time $t = 0$ the rate is instantaneously increased to $k_{ap} = 0.10\ s^{-1}$, $k_{ap} = 0.15\ s^{-1}$, $k_{ap} = 0.20\ s^{-1}$, or $k_{ap} = 0.30\ s^{-1}$: the values correspond to just below the OFF threshold, between the two thresholds, just above the ON threshold, and significantly (~2×) higher than the ON threshold, respectively. Figure 4B depicts the response to an instantaneous decrease in the autophosphorylation rate: the system is initially in the steady state corresponding to $k_{ap} = 0.30\ s^{-1}$, and at $t = 0$ this rate is decreased to $k_{ap} = 0.20\ s^{-1}$, $k_{ap} = 0.15\ s^{-1}$, $k_{ap} = 0.10\ s^{-1}$, or $k_{ap} = 0.05\ s^{-1}$. The computed response times indicate that the monostable system displays similar response times regardless of the amplitude for the input signal. If the value for the dissociation constant of the reaction SK.RR → SK + RR is increased, then the transient time of the system becomes responsive to the strength of the input signal. The temporal responsiveness is much more sensitive for the bistable system, for which the response times are significantly affected by the amplitude of the input signal. The response is very slow for values of the input signal that are just outside of the bistability range ($k_{ap} = 0.20\ s^{-1}$ for the ON kinetics and $k_{ap} = 0.10\ s^{-1}$ for OFF). The response slows down further as the values of k_{ap} approach the threshold values (Fig. 4A and B). We conclude that when the input signal changes instantaneously, the bistable system is slower than the monostable system when the signal values just cross the thresholds of bistability but faster otherwise. Another feature worthy of comment is the independence of response time from the signal strength in the monostable system. One may hypothesize that this would be advantageous when it is physiologically important to provide a constant filter for transient signals irrespective of their amplitude.

One might argue, however, that for gradual changes in the input signal, the responsiveness of the two designs

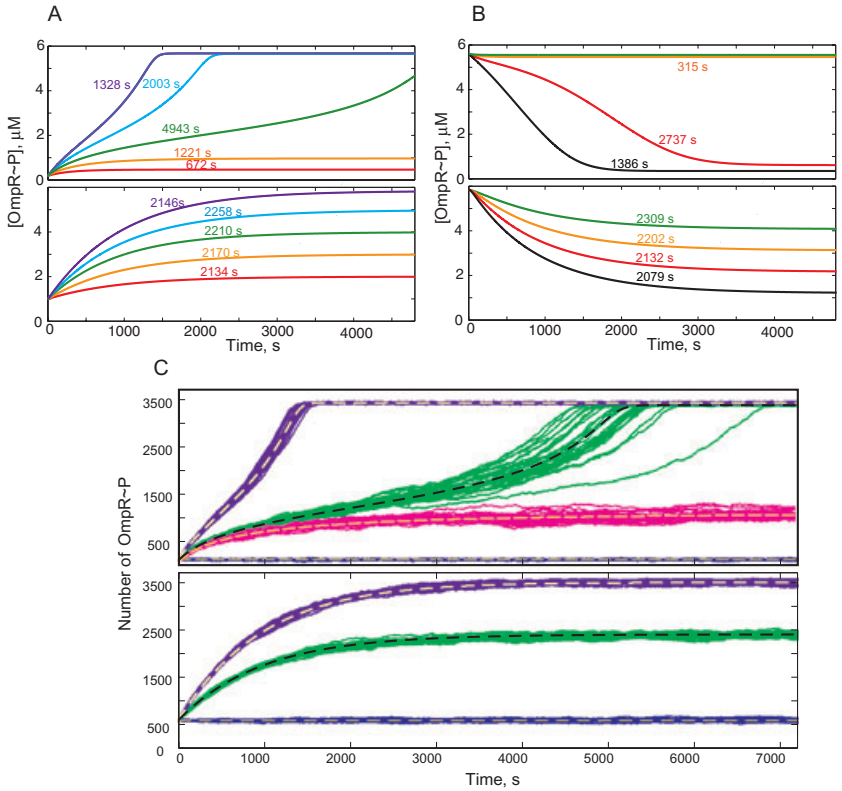

Fig. 4. Dynamic response of bistable (top panel) and monostable (bottom panel) TCS in response to an instantaneous change of the autophosphorylation rate.
A. At time $t = 0$ the rate is instantaneously increased from $k_{ap} = 0.05\ s^{-1}$ to $k_{ap} = 0.10\ s^{-1}$ (red), $k_{ap} = 0.15\ s^{-1}$ (orange), $k_{ap} = 0.20\ s^{-1}$ (green), $k_{ap} = 0.25\ s^{-1}$ (blue), or $k_{ap} = 0.30\ s^{-1}$ (purple).
B. At time $t = 0$ the rate is instantaneously decreased from $k_{ap} = 0.30\ s^{-1}$; the black line represents the case in which $k_{ap} = 0.05\ s^{-1}$ and the other colours are the same as in (A). The numbers are switching times at which 90% of the steady-state response is achieved.
C. Stochastic trajectories following an instantaneous increase from $k_{ap} = 0.05\ s^{-1}$ to $k_{ap} = 0.178\ s^{-1}$ (magenta), $k_{ap} = 0.25\ s^{-1}$ (green), or $k_{ap} = 0.30\ s^{-1}$ (purple). The results for 30 individual runs are plotted in each case. The dashed lines are computed from the deterministic model. We assume a cell volume of 10^{-15} l so that a 1 μM concentration corresponds to 602 molecules.

might change because the full-scale response of the bistable system does not start before the threshold is reached. To investigate this situation we decided to analyse the temporal responsiveness to gradually increasing input signals (Appendix B). We investigated how the graded (monostable) and hysteretic (bistable) designs of TCS respond to a triangular input (linear increase of the autophosphorylation rate followed by a linear decrease in that same rate, Fig. A2) and a sinusoidal input (periodic changes of the autophosphorylation rate). The results of the simulations confirm our conclusions from Figs 4A and B: the bistable design responds faster unless the input signal amplitude is close to the switching threshold.

Stochasticity in the bistable and monostable designs

The simulations performed so far were based on a deterministic (continuous) approximation to chemical kinetics that describes average properties of the system. However, fluctuations in the amount of proteins that are present at very low copy number may lead to stochastic effects that are not well reproduced using a mean-field approach (Kaern *et al.*, 2005). The total number of participating proteins in the EnvZ/OmpR system is relatively large (about 3500 molecules of OmpR and 100 molecules of EnvZ; Cai and Inouye, 2002), but we expect that stochastic effects may still be important in the bistable design, where fluctuations can result in spontaneous switching between two steady states.

Stochastic trajectories were computed by using a Gillespie algorithm for the reactions and parameters summarized in the *Modeling procedures* section. Figure 4C shows trajectories of the stochastic simulations for both TCS, the monostable and the bistable, when the input signal increases (OFF → ON). Three different sizes of step increase in the autophosphorylation rate are shown. We start our simulations at the steady state with $k_{ap} = 0.05\ s^{-1}$ (blue lines) and increase the SK phosphorylation rate to $k_{ap} = 0.178\ s^{-1}$ (magenta lines), $k_{ap} = 0.20\ s^{-1}$ (green lines) or $k_{ap} = 0.30\ s^{-1}$ (purple). Thirty sample trajectories are plotted in each case. Dashed lines show results from deterministic simulations with the same values for the parameters.

Several conclusions are evident from the analysis of the trajectories. (i) Stochastic effects are not important for most parameter values; they lead to small amplitude fluctuations around the mean given by the deterministic approach. (ii) Stochastic effects are most noticeable in the bistable switch and when the EnvZ autophosphorylation rate is just above the switching threshold. Switching times are highly variable under these conditions. (iii) The probability of spontaneous switching due to intrinsic noise is very low. Even when the autophosphorylation rate of the SK is just 1% below the ON threshold (magenta lines in

top panel of Fig. 4C) the amplitude of the fluctuations is not sufficient to cause spontaneous switching. Additional stochastic simulations (not shown) indicate that the probability of spontaneous switching between OFF and ON is below 0.2% for a 3 h time window. (iv) For values of the parameters outside the range in which bistability exists, the magnitude of the fluctuations in the steady-state response is slightly lower for the TCS with the bistable design.

It should be noted that the stochastic simulations shown on Fig. 4C were performed with fixed total copy numbers of SK and RR proteins: we did not include transcription, translation and protein degradation in our model. These additional reactions could affect the noise level and switching probabilities of the model (possibly, on a longer time scale).

Discussion

Intuitive explanation for bistability

A classic bifunctional TCS cannot show bistability, unless an independent Ph that acts upon the phosphorylated RR is present. A classic monofunctional TCS can show a bistable response on a post-translational level. What is the underlying mechanism for this bistability? It is impossible to explain bistability definitively without a rigorous mathematical or numerical analysis of the equations that govern the dynamic behaviour of the system. This analysis can, however, be translated into real biological components and interactions that constitute a mechanism capable of exhibiting bistability.

One requirement for the existence of bistability is the formation of a dead-end complex between the unphosphorylated forms of SK and RR. Our structural analysis of the EnvZ/OmpR TCS suggests that binding of the unphosphorylated RR (OmpR) to one subunit of the SK (EnvZ) dimer may protect the His residue of this subunit from *trans*-autophosphorylation by the other subunit. If this is the case, then a dead-end complex will be formed; its dissociation is required in order to resume the cycle of SK autophosphorylation → phosphotransfer to RR → dephosphorylation of RR. Moreover, the formation of this complex is self-enhancing, thereby creating a positive feedback loop. The more SK.RR complex formed, the smaller the fraction of phosphorylated RR. In turn, the smaller the fraction of phosphorylated RR, the higher the probability that unphosphorylated RR binds to an unphosphorylated SK prior to autophosphorylation of the SK, thereby forming more dead-end complex.

This positive feedback loop leads us to the second requirement for the existence of bistability: dead-end complex formation should affect the phosphatase reaction less than the autophosphorylation reaction. Otherwise, if the SK is bifunctional, this positive feedback loop will be counteracted by a negative feedback loop: the formation of the dead-end complex also decreases the amount of unphosphorylated SK available to dephosphorylate RR~P. If no alternative Ph is present and if spontaneous dephosphorylation of RR~P is much slower than SK-enhanced dephosphorylation of RR~P, then the two feedback loops exactly counteract one another. Thus, a pathway for RR~P dephosphorylation that carries a large fraction of the dephosphorylation flux and is independent of the SK also is required for the existence of bistability.

Our simulations indicate that formation of the SK.RR complex does not affect the concentration of RR~P in the bifunctional system. This observation is consistent with the results of Batchelor and Goulian (2003). Although their model did not include formation of the SK.RR complex, they also found that the concentration of RR~P is not sensitive to the total concentration of SK if [SK] << [RR]. The formation of the dead-end complex in our model decreases the effective concentration of SK, but this decrease does not affect the systemic output RR~P. We note that when a strong alternative Ph is present, the contribution of the negative feedback loop created by the formation of the dead-end complex is diminished. Therefore, although a bifunctional SK is capable of achieving a bistable response (data not shown), the system is effectively monofunctional because the phosphatase activity of SK is insignificant.

Physiological consequences of bistability

At the population level, hysteretic bistability has three fundamental physiological consequences. (i) Hysteric switches tend to display ALL-or-NONE steady-state output characteristics. This means that precise continuous tuning of the systemic output to environmental input is not possible. Therefore, we do not expect to see bistability in TCS that are required to respond continuously to a wide range of environmental conditions through a continuous variation of cellular gene expression. Consistent with this idea, bifunctionality of the SK EnvZ prevents bistability in the EnvZ/OmpR system. On the other hand, such ALL-or-NONE responses might be important for developmental switches that require in a digital (yes or no) commitment to differentiation. (ii) The existence of two different switching thresholds and bistability between these can lead to irreversible transitions between the two stable steady states in response to transient signals. Again, such a design would be deleterious if a graded response were required of the sensor, but may be advantageous for switches controlling differentiation and development. (iii) The slow response of bistable switches to signals having amplitudes near the switching threshold allows for filtering of transient fluctuations that otherwise would lead to transi-

tions that could be either physiologically detrimental or metabolically very costly. On the other hand, outside the range of bistability, these systems exhibit a fast response to changes in input signal and a fast recovery from spurious fluctuations in the phosphorylation level of its proteins.

Additionally, the existence of bistability has consequences on a single-cell level. Bistability implies that, within a given population of cells and for a new signal, two alternative states may coexist. It is hard to imagine a situation in which this type of response could have evolved for systems in which a decisive adaptation of the cell to a new state is fundamental for immediate survival (such as osmotic stress). In such a situation, a homogeneous response of the population is expected to maximize survival and therefore bistability should be deleterious. However, one can imagine a situation in which the cell is repeatedly subjected to large changes in the environment, requiring a large and rapid shift in metabolism to ensure survival. Spontaneous transitions that are uncorrelated with the environmental signal in a fraction of the population may be a beneficial strategy when changes in the environment are random and fast (Thattai and van Oudenaarden, 2004; Kussell and Leibler, 2005). Multistable switches in general allow noise-driven transitions between steady states. However, our stochastic simulations reveal a low probability of stochastic transition between the two steady states that result from post-translation regulation in TCS. This observation is in agreement with the observation that transcription is the major source of noise in bacteria (Thattai and van Oudenaarden, 2001; Ozbudak *et al.*, 2002; Kaern *et al.*, 2005). Accordingly, we expect that population-level effects of bistability in TCS will be of the most physiological relevance.

Biological relevance of bistability in two-component systems

Batchelor *et al.* (2004) have demonstrated a graded response for the EnvZ/OmpR TCS. Our model of the system predicts the same type of behaviour, but only when the dephosphorylation of the RR that is independent of the SK phosphotase is insignificant. The autophosphatase activity of OmpR is small (Qin *et al.*, 2001) and no alternative Ph acting on OmpR has been reported. However, alternative views on the role of EnvZ in the dephosphorylation of OmpR~P have been expressed in the literature. Mattison and Kenney (2002) suggested that the affinity of OmpR~P and EnvZ is small and that there is an alternative Ph that acts on OmpR~P *in vivo*. However, subsequent findings by Yoshida *et al.* (2002a,b) questioned these conclusion and presented evidence that both phosphorylated and unphosphorylated forms of OmpR interact strongly with EnvZ and with similar affinities. We view our predictions regarding the interactions within the TCS that are required for bistability, taken together with the graded response of the EnvZ/OmpR system shown by Batchelor *et al.* (2004), as further evidence against the existence of an alternative Ph for OmpR~P. Moreover, our results illustrate an additional role for the bifunctional design in TCS – to ensure a graded system response over large signal variation regardless of dead-end complex formation.

Are there TCS in which post-translational bistability can take place? We conducted a literature survey of TCS, for which their biochemistry has been characterized (Table S1). Few of these are characterized in full detail. Those with the most extensive determination of their parameters are the CheA/CheY system (Baker *et al.*, 2006), the NtrB/NtrC system (Jiang *et al.*, 2000a,b; Pioszak and Ninfa, 2003), the Spo0 system (Piggot and Hilbert, 2004), and the VanS/VanR system (Wright *et al.*, 1993; Fisher *et al.*, 1996). The data available for these and other TCS (Kato and Groisman, 2004) suggest that the equilibrium and rate constants for the corresponding reactions in different classical TCS are very similar and mostly within an order of magnitude. A recent survey of all the TCS for *E. coli* provides further support for this claim (Yamamoto *et al.*, 2005). Several of the well-characterized TCS – NtrB/NtrC, VanS/VanR, PmrD/PmrB – are bifunctional with no alternative Ph and are therefore not expected to show post-tran bistability. However, the NtrB/NtrC system includes a third protein whose regulatory role is important, so a more complex model needs to be built in order to fully analyse the possibility of bistability for this TCS.

Our simulations suggest that bistability is possible when there is cross-talk between two bifunctional TCS. For example, the SK, VanS, from *Enterococci* has been demonstrated *in vitro* to interact not only with its cognate RR, VanR, but also with the RR, PhoB, from *E. coli* (Fisher *et al.*, 1996). In our computer model of this system (not shown), the dead-end complex that PhoB forms with VanS is able to sequester VanS from the VanS–VanR phosphorylation cycle, thus creating a positive feedback loop similar to the one discussed above. Furthermore, PhoB can also interact with its cognate bifunctional SK, PhoR, which provides an alternative to the VanS pathway for PhoB dephosphorylation. However, we must stress that this model was set up on the basis of *in vitro* experiments with proteins from different bacteria (Fisher *et al.*, 1996). Thus, the VanS/PhoB interaction is unlikely to be physiologically meaningful *in vivo*. Nevertheless, these simulations suggest that a TCS that is similar to this may be an adequate initial design for building a synthetic TCS that acts as a bistable switch.

Table S1 summarizes our survey of TCS for which kinetic and bifunctionality information exists in the literature. We include an analysis regarding the plausible

detection of bistability in the different TCS based upon the existence of SK bifunctionality, upon the existence of Ph for the RR that are independent of the SK, and upon the function of the TCS. The TCS with a plausible possibility of post-translational bistability can be divided into three groups according to their physiological function. Some of the TCS function as environmental sensors (for example, PhoR/PhoP in *B. subtilis*, BaeS/BaeR in *E. coli,* and SphS/SphR in *Synechocystis*); these are not likely to benefit from bistability as continuous and reversible sensing is expected. Other TCS (for example, YycG/YycF and the phosphorelays DivJ/DivK and PleC/PleD in *B. subtilis*) are involved in differentiation and cell cycle transitions – functions that benefit from bistable hysteretic switching. The remaining TCS control virulence or growth in particular environments (for example VirA/VirG in *Agrobacterium tumefaciens*, CreC/CreB, NarX/NarL, NarQ/NarP and YehU/YehT in *E. coli*, and PrrB/PrrA in *Mycobacterium tuberculosis*). These TCS will benefit from bistable switching if controlled lifestyle changes are differentiation-like transitions. Intriguingly, several experimental studies suggest bistability in the VirA/VirG system of *A. tumefaciens* (Brencic *et al.*, 2005; Goulian and van der Woude, 2006). However, it is not known whether bistability in this system is due to a post-translational mechanism or if it involves autocatalytic transcriptional feedbacks.

Another possibility of finding TCS for which bistability is physiologically relevant is among the group of monofunctional TCS. In these systems, dephosphorylation of the RR is independent of the SK, which fulfils one of the requirements for bistability. The other requirement that must be met is the formation of a dead-end complex between the dephosphorylated SK and the RR. One of the best characterized monofunctional TCS controls bacterial chemotaxis; this system includes, among other molecules, the SK, CheA, the RRs CheY and CheB and the phosphatase CheZ (Baker *et al.*, 2006). However, based on structural analysis it is unlikely that CheA–CheY will be a dead-end complex. Indeed, the RR, CheY, binds a specialized domain of the kinase CheA; seven structures for this complex have been reported (entries 1UOS, 1BDJ, 1EYA, 1FFW, 1AO0, 1FFG and 1FFS of the Protein Data Bank, PDB). Another domain of CheA, denoted Hpt, contains a His residue that is autophosphorylated (entries 1TQG, 1B3Q and 1I5N of the PDB). The long stretch of approximately 50 amino acids that connects the Hpt domain to the CheY binding domain has not been crystallized, and it contains two Pro residues. Using the Phyre web server (Kelley *et al.*, 2000), we predict that one of these two residues (Pro132) is in a region expected to be disordered (data not shown). It is conceivable that this disordered loop around Pro132 can act as a hinge that allows the Hpt domain to swing between the CheA catalytic domain and the CheY binding domain. If this were so, then binding of CheY would not prevent phosphorylation of the CheA Hpt domain and no dead-end complex would form.

Bistability could be physiologically desirable in TCS that are used for the realization of a developmental switch. In fact, it has been shown that bistability occurs in sporulating populations of *B. subtilis* (Maamar and Dubnau, 2005; Veening *et al.*, 2005). Spore formation is a costly cell fate decision in response to severe nutrient depletion or other extreme challenges in the environment. The existence of heterogeneity in an isogenic population of cells under these conditions leads to several adaptive strategies that are beneficial for genotype survival (see Dubnau and Losick, 2006 for a review). This sporulation process is regulated by a non-classical TCS, the Spo phosphorelay, in which four steps of phosphate transfer occur, eventually resulting in phosphorylation of the RR, Spo0A. Intriguingly, deletion of the Spo0E phosphatase that acts directly on Spo0A abolishes bistability (Veening *et al.*, 2005). However, several other auto-stimulatory loops affecting transcription and phosphorylation of Spo0A have been reported (Strauch *et al.*, 1992; Strauch and Hoch, 1993; Fujita and Sadaie, 1998). Therefore, no conclusive inference can be made regarding the role of the 'dead-end' complex mechanism for Spo0AP bistability. In many bacteria, such as *Myxococcus xanthus* or *Caulobacter crescentus,* multiple TCS are associated with development, cell cycle progression and differentiation (Skerker *et al.*, 2005; Biondi *et al.*, 2006; Goldman *et al.*, 2006; Holtzendorff *et al.*, 2006; Pierce *et al.*, 2006; Ueki and Inouye, 2006). We believe that these TCS are likely candidates to exhibit the proposed mechanism of bistability. We suggest that investigations of the complex between the unphosphorylated SK and RR, and of the potential RR~P dephosphorylation reactions that are independent of the SK are key to determining the plausibility of a bistable response for any given TCS.

Suggested experimental tests

Based on the preceding subsection we expect that our suggested bistability mechanism may be applicable to some naturally occurring TCS. Table S1 analyses several candidate systems and pinpoints the cases in which bistability might be possible. Experimental work is required to find out whether bistability exists or not in these systems. Below we suggest possible generic guidelines to *in vitro* and *in vivo* experiments that can be used to verify the existence of bistability. However, specific experimental-procedures will certainly depend on the details of the particular TCS.

i Existence of a long-lived complex between unphosphorylated SK and RR, in which RR interferes with

phosphorylation of the SK subunit to which it is bound, is crucial for bistability to exist. To test for existence of the dead-end complex *in vitro* we suggest measuring the autophosphorylation flux of the SK (e.g. by following hydrolysis of radioactive ATP) after pre-incubation with increasing amounts of the cognate RR. If the RR binds SK forming a dead-end complex, then the rate of SK autophosphorylation will be slower with increasing concentrations of RR.

ii *In vitro* reconstructed TCS can also be used to test for bistability by: (i) measuring the steady-state concentration of phosphorylated RR (if stable and reliably detectable), or (ii) measuring the flux of ATP hydrolysis as function of signals that modulate kinase and/or phosphatase activity of SK. If the physiological signal is unknown or unusable, it may be possible to modulate the kinase activity by varying the ATP/ADP ratio, by addition non-hydrolyzable ATP analogues to serve as competitive inhibitors or by varying the concentrations of Mg2+ ions, using chelating agents such as EDTA. If the TSC is bistable, the model predicts that different steady states for the system can be observed depending on whether most of the RR is initially phosphorylated or unphosphorylated. Note that this *in vitro* system is only likely to display bistability if the alternative Ph is purified and included in the assay or if the RR possesses significant autophosphotase activity.

iii If the natural inducing signal of a TCS is known, an *in vivo* assay for bistability can be set up by monitoring the expression of genes under RR~P control as a function of inducer concentration. If the mean expression levels of the relevant genes is different between cells that were initially pre-induced and cells that were not pre-induced, then bistability is present. Moreover, a bimodal population distribution of expression levels is expected to be observed for inducer concentrations near the switching threshold.

iv Our model predicts that TCS are likely to display a graded response, unless an alternative (to SK) pathway that dephosphorylates RR exists. However, we foresee that introducing an additional Ph in the system will allow re-engineering of the system response. For example, one can imagine introducing an additional mutated copy of the SK gene in the bacterial genome. The mutated SK would have only phosphatase activity. Such a re-engineered system may show a bistable response if a long-lived SK.RR complex is formed.

Conclusions and predictions

Using the EnvZ/OmpR TCS as an example we have used structural modelling and *in silico* protein docking to analyse the potential binding of the SK (EnvZ) to the RR (OmpR). Our analysis suggests that conformational changes must occur in the SK between recurring *trans*-autophosphorylation and phosphotransfer reactions. In order for the phosphotransfer to occur, the RR must bind the dimer in such a way that the catalytic domain of the SK is unable to access its phosphorylatable His residue, thus effectively preventing His phosphorylation whenever the RR is bound. This also may lead to the formation of a dead-end complex between the SK and the RR if the conformational change of the SK is as dependent on the binding of the RR as it is on the autophosphorylation of the His residue. The formation of such a dead-end complex would be self-enhancing and would result in bistability for the monofunctional system. However, bistability is not possible when the RR is mainly dephosphorylated by the unphosphorylated SK, as in the case of EnvZ/OmpR system. Our analysis identifies three conditions that are necessary for the existence of bistability in classical TCS: (i) there must be a high affinity complex between the unphosphorylated RR and the SK; (ii) formation of this complex must prevent autophosphorylation of the RR; and (iii) the largest fraction of the RR desphosphorylation flux must be independent of the dephosphorylated SK.

Modeling procedures

Reactions and kinetics

The set of reactions from Fig. 1C and their mass-action rate constants used for our simulations are given in Table 1. The mechanistic model used in this work builds on the kinetic scheme proposed by Batchelor and Goulian (2003), and extends it in several important aspects:

i We introduce the Ph in order to model generic monofunctional or bifunctional TCS in which there is an additional Ph enzyme that is capable of dephosphorylating the RR. Reactions #11–13 (Table 1) describe the interaction of this Ph with the RR. The model of Batchelor and Goulian (2003) specifically addressed the EnvZ/OmpR system for which no alternative Ph has been found; therefore, their model did not include these reactions.

ii We explicitly include the dead-end complex SK.RR of unphosphorylated SK and RR (reactions # 9–10, Table 1). Such a complex has been shown to exist and to be relatively long-lived for a number of TCS, including EnvZ/OmpR. Moreover, this complex is presumably formed following the catalytic phosphatase transformation and phosphate release from the SK.RR~P (reaction #8, Table 1). The model of Batchelor and Goulian (2003) grouped reactions 8 and 9 into one step and excluded the possibility of reaction #10.

iii We explicitly include the complex SK.RR~P as a product of the kinase reaction (#5, Table 1). The model of Batchelor and Goulian (2003) included this complex for modelling the phosphatase reaction but assumed its instant dissociation after the kinase reaction.

While addressing the design of generic TCS we choose parameter value based on the *in vitro* biochemical measurements for the EnvZ/OmpR system. The rationale for estimation of parameter values is given below:

i For the results shown in Figs 2–4 and in Table 1 we chose not to include the autophosphatase reaction of the RR (RR~P → RR). For OmpR~P, the spontaneous dephosphorylation rate has been measured and found to be very low (half-life is over 1 h; Qin *et al.*, 2001). This value is consistent with the dominant role of EnvZ in OmpR dephosphorylation. For monofunctional designs, the existence of spontaneous dephosphorylation instead of or in addition to dephosphorylation by an alternative Ph still allows for bistable behaviour (data not shown). However, saturation of the Ph enlarges the bistability region.

ii Reported affinity measurements (Cai and Inouye, 2002; Yoshida *et al.*, 2002a,b) provide estimates of approximately 1 μM for the equilibrium dissociation constants of EnvZ–OmpR and EnvZ–OmpR~P complexes. Taking the typical association constant of protein complexes in the cell to be on the order of 1 μM s^{-1}, and using a factor of 0.5 to account for the fact that that only OmpR is freely diffusible while EnvZ has a *trans*-membrane domain, we estimate the dissociation constants to be around 0.5 s^{-1}. For the monofunctional design, we decrease the affinity of EnvZ and OmpR by decreasing 10-fold the association constant to 0.05 μM s^{-1}.

iii There is limited data on the phosphotransfer rate of the EnvZ/OmpR system. We used the measurements of Fisher *et al.* (1996) for the phosphotransfer from the SK, VanS, to its cognate RR, VanR (1.5 s^{-1}). This value is consistent with the nearly complete phosphotransfer that is observed by the first time point (20 s) of the phosphotransfer assay by Qin *et al.* (2001).

iv The half-life of OmpR~P in the presence of EnvZ was estimated to be 30 s by Qin *et al.* (2001). However, in their experimental essay the concentration of OmpR~P was 0.2 μM, indicating that only 20% of it will be in the complex with EnvZ. We therefore estimate the phosphatase rate constant to be k_{ph}~(1/0.2)*log(2)/30 = 0.05 s^{-1}.

v Concentrations for EnvZ and OmpR were computed using the data of Cai and Inouye (2002) and assuming a cell volume of 10^{-15} l. Even though the data indicate that the total concentration of both proteins increases during osmotic stress, we ignore this effect for simplicity.

Network cooperativity, additional states and conformations

We emphasize that in this work we aimed at constructing the most generic and simplified model of a TCS that is still capable of showing bistability. This approach (i) creates a model that is tractable for theoretical and computational analysis, (ii) reduces the number of assumptions about unknown parameters, and (iii) leads to an intuitive understanding of what is mechanistically required for bistability to occur. Mechanistically more detailed models for TCS may be needed if one is interested in fine-tuning the parameter conditions under which bistability may be observed. However, these simplified models guide and inform us regarding where to start looking for bistability, if more detailed models are required. Below we discuss some of our simplifying assumptions in details and what implications they have for our conclusions.

First, for reasons of simplicity, our model (as well as that of Batchelor and Goulian, 2003) does not consider cooperativity in the signal transduction process of the TCS. A consequence of this is that binding of RR to one SK subunit does not affect (i) autophosphorylation of the other SK subunit, (ii) phosphotransfer between SK and RR, or (iii) autodephosphorylation of the SK. In addition, the phosphorylation of one SK subunit is independent of the phosphorylation state of the other SK subunit. Although evidence for cooperativity in the autophosphorylation of SKs is lacking for most TCS, published data supports that such cooperativity exists in the Ntr and in the Che systems (Levit *et al.*, 1996; Jiang *et al.*, 2000b). Although cooperativity may change the regions of bistability in parameter space, not considering such cooperativity explicitly will not affect the qualitative behaviour of the models (and thus our conclusions). To illustrate this point we repeated our analysis on several generalized models that explicitly consider SK as a dimer, introducing cooperativity and asymmetry in the phosphorylation of the two SK subunits (Fig. S4 and its caption).

Second, the model does not explicitly consider ATP/ADP binding and dissociation reactions. These reactions are usually fast compared with the catalytic steps of the process, which justifies the quasi-equilibrium assumption. Effects of varying nucleotide concentrations can still be investigated through their modulation of the effective rate for the kinase reaction. Similarly, the model does not explicitly account for alternative conformational states of the network proteins, because we assume conformational dynamics to be fast, thus generating pools of proteins in conformational equilibrium. For example, it has been suggested (Jin and Inouye, 1993; Stock *et al.*, 2000; Cai and Inouye, 2003; Pioszak and Ninfa, 2003) that unphosphorylated SK can adopt two alternative conformations one with high kinase activity another with high autophosphatase activity. The equilibrium constant K_{eq} or transition rates between these two states can serves as a physiological signal for TSC activation. Assuming that the equilibrium constant is independent of the RR binding state, and that conformational transitions are fast, the ratio of kinase and phosphatase forms is given by

$$\frac{[SK^{ph}]}{[SK^{kin}]} = K_{eq}; \quad [SK^{ph}] \propto \frac{K_{eq}}{1+K_{eq}}; \quad [SK^{ph}] \propto \frac{1}{1+K_{eq}};$$

Assuming that when 100% of SK is in the kinase form, the autophosphorylation rate is at its maximal value k_{ap}^{max} and the phosphatase rate is negligible; in the same fashion, when 100% of SK is in the phosphatase form, the phosphatase rate is at its maximal value k_{ph}^{max} and the autophosphorylation rate is negligible. These assumptions allow us to derive the following relation among the reaction rates:

$$k_{ap} = k_{ap}^{max}(1 - k_{ph}/k_{ph}^{max})$$

This model was used to compute the response of the system to changes of both phosphatase and autophosphorylation rates in Fig. 2C. The model that explicitly accounts for the two SK conformations yields similar conclusions (data not shown).

Structural analysis

The structural modelling of EnvZ was based on the crystallized structure for the two cytoplasmatic domains of the protein (entries 1JOY and 1BXD from the PDB; Berman *et al*., 2007). The two separate domains were assembled in alternative conformations that allow for transphosphorylation of His 243 in the dimer of the protein and that take into account experimental information regarding residues that are in contact between subunits. The monomers were then assembled as a dimmer using the co-ordinates in the PDB entry 1JOY. The structural model for the phosphorylation domain of OmpR was done using SPDBViewer and the Swiss model service (Schwede *et al*., 2003; Arnold *et al*., 2006). PDB entries 1KGS and 1P2F were used to obtain a model of the RR domain of OmpR. The same entries were then used to assemble the OmpR RR domain to its DNA binding domain (PDB entry 1ODD). SPDBViewer was used for loop reconstruction, structure optimization and energy minimization of the models. Four rounds of energy minimization were run for each protein. Docking of OmpR to the EnvZ dimer models was done using Hex 4.5 (Ritchie, 2003).

Bistability boundaries

We have solved the steady-state equations for both bifunctional and the monofunctional systems. These equations can be reduced to a third-degree degree polynomial in [RR~P], if one assumes that $[RR]_{total} >> [SK]_{total}$. The discriminant of a third-degree polynomial equation must be zero if the equation is to have three positive roots. For bistability to exist, our system needs to have three positive steady-state solutions, two stable and one unstable. This discriminant can be expressed as function of the following system parameters:

- k_{ap}, rate of autophosphorylation
- k_{ph}, rate of dephosphorylation (bifunctional SK, Figs. S1 and S2)
- $K_{de} = k_{d3}/k_{b3}$, dissociation constant of the SK.RR dead-end complex
- $K_{pt} = (k_{d1} + k_{pt})/k_{b1}$, Michaelis–Menten constant of the phosphotransfer reaction
- k_{pt}, catalytic rate of the phosphotransfer reaction
- $K_2 = k_{d2}/k_{b2}$, dissociation constant of the SK.RR~P complex
- k_{b2}, binding rate of SK to RR~P
- $K_m = (k_{d4} + k_{cat})/k_{b4}$, Michaelis–Menten constant of the phosphatase reaction
- $V_{max} = k_{cat}[Ph]_{total}$, Michaelis–Menten V_{max} of the phosphatase reaction
- $[SK]_{total}$, total concentration of SK
- $[RR]_{total}$, total concentration of RR

By equating the discriminant to 0 we determine the boundaries of the bistable region, as well as the region in which this bistability is physically realizable (that is $0 < [RR\sim P] < [RR]_{total}$). Then, we computed parameter values as in Table 1, and plotted the region of parameter space in which each system is bistable. The results are shown in Fig. 3, Figs S1 and S2; each physically realizable region of bistability is shaded in grey for each two-dimensional section of parameter space. The *x*-axis in these plots corresponds to one of the input parameters (k_{ap} – Fig. 3, or k_{ph} – Figs S1 and S2) and the *y*-axis corresponds to one of the other parameters.

Acknowledgements

The authors are grateful to A.Y. Mitrophanov for useful comments. We appreciate the insightful comments and helpful suggestions of the anonymous reviewers and thank them for helping improve the work. This work was supported by a Whitaker Foundation start-up fund to O.A.I., by a Ramon y Cajal award and by grant BFU 2007-62772/BMC from the Spanish MCT to R.A. and by a grant from the US Public Health Service (RO1-GM30054) to M.A.S.

References

Ajo-Franklin, C.M., Drubin, D.A., Eskin, J.A., Gee, E.P., Landgraf, D., Phillips, I., and Silver, P.A. (2007) Rational design of memory in eukaryotic cells. *Genes Dev* **21:** 2271–2276.

Alves, R., and Savageau, M.A. (2003) Comparative analysis of prototype two-component systems with either bifunctional or monofunctional sensors: differences in molecular structure and physiological function. *Mol Microbiol* **48:** 25–51.

Angeli, D., Ferrell, J.E., Jr, and Sontag, E.D. (2004) Detection of multistability, bifurcations, and hysteresis in a large class of biological positive-feedback systems. *Proc Natl Acad Sci USA* **101:** 1822–1827.

Arnold, K., Bordoli, L., Kopp, J., and Schwede, T. (2006) The SWISS-MODEL workspace: a web-based environment for protein structure homology modelling. *Bioinformatics* **22:** 195–201.

Atkinson, M.R., Savageau, M.A., Myers, J.T., and Ninfa, A.J. (2003) Development of genetic circuitry exhibiting toggle switch or oscillatory behavior in *Escherichia coli*. *Cell* **113:** 597–607.

Baker, M.D., Wolanin, P.M., and Stock, J.B. (2006) Signal transduction in bacterial chemotaxis. *Bioessays* **28:** 9–22.

Batchelor, E., and Goulian, M. (2003) Robustness and the cycle of phosphorylation and dephosphorylation in a two-component regulatory system. *Proc Natl Acad Sci USA* **100:** 691–696.

Batchelor, E., Silhavy, T.J., and Goulian, M. (2004) Continuous control in bacterial regulatory circuits. *J Bacteriology* **186:** 7618–7625.

Becskei, A., Seraphin, B., and Serrano, L. (2001) Positive feedback in eukaryotic gene networks: cell differentiation by graded to binary response conversion. *EMBO J* **20:** 2528–2535.

Beier, D., and Gross, R. (2006) Regulation of bacterial virulence by two-component systems. *Curr Opin Microbiol* **9:** 143–152.

Berman, H., Henrick, K., Nakamura, H., and Markley, J.L. (2007) The worldwide Protein Data Bank (wwPDB): ensuring a single, uniform archive of PDB data. *Nucleic Acids Res* **35:** D301–D303.

Biondi, E.G., Skerker, J.M., Arif, M., Prasol, M.S., Perchuk, B.S., and Laub, M.T. (2006) A phosphorelay system controls stalk biogenesis during cell cycle progression in *Caulobacter crescentus*. *Mol Microbiol* **59:** 386–401.

Brencic, A., Angert, E.R., and Winans, S.C. (2005) Unwounded plants elicit *Agrobacterium vir* gene induction and T-DNA transfer: transformed plant cells produce

opines yet are tumour free. *Mol Microbiol* **57:** 1522–1531.
Cai, S.J., and Inouye, M. (2002) EnvZ–OmpR interaction and osmoregulation in *Escherichia coli*. *J Biolog Chem* **277:** 24155–24161.
Cai, S.J., and Inouye, M. (2003) Spontaneous subunit exchange and biochemical evidence for trans-autophosphorylation in a dimer of *Escherichia coli* histidine kinase (EnvZ). *J Mol Biol* **329:** 495–503.
Cai, S.J., Khorchid, A., Ikura, M., and Inouye, M. (2003) Probing catalytically essential domain orientation in histidine kinase EnvZ by targeted disulfide crosslinking. *J Mol Biol* **328:** 409–418.
Calva, E., and Oropeza, R. (2006) Two-component signal transduction systems, environmental signals, and virulence. *Microbial Ecol* **51:** 166–176.
Craciun, G., Tang, Y., and Feinberg, M. (2006) Understanding bistability in complex enzyme-driven reaction networks. *Proc Natl Acad Sci USA* **103:** 8697–8702.
Dubnau, D., and Losick, R. (2006) Bistability in bacteria. *Mol Microbiol* **61:** 564–572.
Ferrell, J.E. (2002) Self-perpetuating states in signal transduction: positive feedback, double-negative feedback and bistability. *Curr Opin Cell Biol* **14:** 140–148.
Fisher, S.L., Kim, S.K., Wanner, B.L., and Walsh, C.T. (1996) Kinetic comparison of the specificity of the vancomycin resistance kinase VanS for two response regulators, VanR and PhoB. *Biochemistry* **35:** 4732–4740.
Fujita, M., and Sadaie, Y. (1998) Feedback loops involving Spo0A and AbrB in in vitro transcription of the genes involved in the initiation of sporulation in *Bacillus subtilis*. *J Biochem* **124:** 98–104.
Gardner, T.S., Cantor, C.R., and Collins, J.J. (2000) Construction of a genetic toggle switch in *Escherichia coli*. *Nature* **403:** 339–342.
Goldman, B.S., Nierman, W.C., Kaiser, D., Slater, S.C., Durkin, A.S., Eisen, J., *et al.* (2006) Evolution of sensory complexity recorded in a myxobacterial genome. *Proc Natl Acad Sci USA* **103:** 15200–15205.
Goulian, M., and van der Woude, M. (2006) A simple system for converting *lacZ* to *gfp* reporter fusions in diverse bacteria. *Gene* **372:** 219–226.
Hoch, J.A., and Varughese, K.I. (2001) Keeping signals straight in phosphorelay signal transduction. *J Bacteriol* **183:** 4941–4949.
Holtzendorff, J., Reinhardt, J., and Viollier, P.H. (2006) Cell cycle control by oscillating regulatory proteins in *Caulobacter crescentus*. *Bioessays* **28:** 355–361.
Huber, R.E., Wallenfels, K., and Kurz, G. (1975) The action of beta-galactosidase (*Escherichia coli*) on allolactose. *Can J Biochem* **53:** 1035–1038.
Igoshin, O.A., Price, C.W., and Savageau, M.A. (2006) Signalling network with a bistable hysteretic switch controls developmental activation of the sigma(F) transcription factor in *Bacillus subtilis*. *Mol Microbiol* **61:** 165–184.
Isaacs, F.J., Hasty, J., Cantor, C.R., and Collins, J.J. (2003) Prediction and measurement of an autoregulatory genetic module. *Proc Natl Acad Sci USA* **100:** 7714–7719.
Jiang, P., Atkinson, M.R., Srisawat, C., Sun, Q., and Ninfa, A.J. (2000a) Functional dissection of the dimerization and enzymatic activities of *Escherichia coli* nitrogen regulator II and their regulation by the PII protein. *Biochemistry* **39:** 13433–13449.
Jiang, P., Peliska, J.A., and Ninfa, A.J. (2000b) Asymmetry in the autophosphorylation of the two-component regulatory system transmitter protein nitrogen regulator II of *Escherichia coli*. *Biochemistry* **39:** 5057–5065.
Jin, T., and Inouye, M. (1993) Ligand binding to the receptor domain regulates the ratio of kinase to phosphatase activities of the signaling domain of the hybrid *Escherichia coli* transmembrane receptor, Taz1. *J Mol Biol* **232:** 484–492.
Jobe, A., and Bourgeois, S. (1972) lac Repressor–operator interaction. VI. The natural inducer of the lac operon. *J Mol Biol* **69:** 397–408.
Kaern, M., Elston, T.C., Blake, W.J., and Collins, J.J. (2005) Stochasticity in gene expression: from theories to phenotypes. *Nat Rev Genet* **6:** 451–464.
Kato, A., and Groisman, E.A. (2004) Connecting two-component regulatory systems by a protein that protects a response regulator from dephosphorylation by its cognate sensor. *Genes Dev* **18:** 2302–2313.
Kelley, L.A., MacCallum, R.M., and Sternberg, M.J. (2000) Enhanced genome annotation using structural profiles in the program 3D-PSSM. *J Mol Biol* **299:** 499–520.
Kobayashi, H., Kaern, M., Araki, M., Chung, K., Gardner, T.S., Cantor, C.R., and Collins, J.J. (2004) Programmable cells: interfacing natural and engineered gene networks. *Proc Natl Acad Sci USA* **101:** 8414–8419.
Kramer, B.P., and Fussenegger, M. (2005) Hysteresis in a synthetic mammalian gene network. *Proc Natl Acad Sci USA* **102:** 9517–9522.
Kussell, E., and Leibler, S. (2005) Phenotypic diversity, population growth, and information in fluctuating environments. *Science* **309:** 2075–2078.
Levit, M., Liu, Y., Surette, M., and Stock, J. (1996) Active site interference and asymmetric activation in the chemotaxis protein histidine kinase CheA. *J Biol Chem* **271:** 32057–32063.
Maamar, H., and Dubnau, D. (2005) Bistability in the *Bacillus subtilis* K-state (competence) system requires a positive feedback loop. *Mol Microbiol* **56:** 615–624.
Maamar, H., Raj, A., and Dubnau, D. (2007) Noise in gene expression determines cell fate in *Bacillus subtilis*. *Science* **317:** 526–529.
Markevich, N.I., Hoek, J.B., and Kholodenko, B.N. (2004) Signaling switches and bistability arising from multisite phosphorylation in protein kinase cascades. *J Cell Biol* **164:** 353–359.
Mascher, T. (2006) Intramembrane-sensing histidine kinases: a new family of cell envelope stress sensors in *Firmicutes bacteria*. *Fems Microbiol Lett* **264:** 133–144.
Mascher, T., Helmann, J.D., and Unden, G. (2006) Stimulus perception in bacterial signal-transducing histidine kinases. *Microbiol Mol Biol Rev* **70:** 910–938.
Mattison, K., and Kenney, L.J. (2002) Phosphorylation alters the interaction of the response regulator OmpR with its sensor kinase EnvZ. *J Biol Chem* **277:** 11143–11148.
Mizuno, T. (1998) His-Asp phosphotransfer signal transduction. *J Biochem* **123:** 555–563.

Mizuno, T. (2005) Two-component phosphorelay signal transduction systems in plants: from hormone responses to circadian rhythms. *Biosci Biotechnol Biochem* **69:** 2263–2276.

Monod, J., and Jacob, F. (1961) General conclusions – teleonomic mechanisms in cellular metabolism, growth, and differentiation. *Cold Spring Harb Symp Quant Biol* **26:** 389–401.

Novick, A., and Weiner, M. (1957) Enzyme induction as an All-or-None phenomenon. *Proc Natl Acad Sci USA* **43:** 553–566.

Ozbudak, E.M., Thattai, M., Kurtser, I., Grossman, A.D., and van Oudenaarden, A. (2002) Regulation of noise in the expression of a single gene. *Nat Genet* **31:** 69–73.

Parkinson, J.S. (2003) Bacterial chemotaxis: a new player in response regulator dephosphorylation. *J Bacteriol* **185:** 1492–1494.

Perego, M., and Hoch, J.A. (1996) Protein aspartate phosphatases control the output of two-component signal transduction systems. *Trends Genet* **12:** 97–101.

Perego, M., Glaser, P., and Hoch, J.A. (1996) Aspartyl-phosphate phosphatases deactivate the response regulator components of the sporulation signal transduction system in *Bacillus subtilis*. *Mol Microbiol* **19:** 1151–1157.

Pierce, D.L., O'Donnol, D.S., Allen, R.C., Javens, J.W., Quardokus, E.M., and Brun, Y.V. (2006) Mutations in DivL and CckA rescue a divJ null mutant of *Caulobacter crescentus* by reducing the activity of CtrA. *J Bacteriol* **188:** 2473–2482.

Piggot, P.J., and Hilbert, D.W. (2004) Sporulation of *Bacillus subtilis*. *Curr Opin Microbiol* **7:** 579–586.

Pioszak, A.A., and Ninfa, A.J. (2003) Mechanism of the PII-activated phosphatase activity of *Escherichia coli* NRII (NtrB): how the different domains of NRII collaborate to act as a phosphatase. *Biochemistry* **42:** 8885–8899.

Ptashne, M. (2004) *A Genetic Switch: Phage Lambda Revisited*. Cold Spring Harbor, NY: Cold Spring Harbor Laboratory Press.

Qin, L., Yoshida, T., and Inouye, M. (2001) The critical role of DNA in the equilibrium between OmpR and phosphorylated OmpR mediated by EnvZ in *Escherichia coli*. *Proc Natl Acad Sci USA* **98:** 908–913.

Ritchie, D.W. (2003) Evaluation of protein docking predictions using Hex 3.1 in CAPRI rounds 1 and 2. *Proteins-Struct Funct Genet* **52:** 98–106.

Russo, F.D., and Silhavy, T.J. (1991) EnvZ controls the concentration of phosphorylated OmpR to mediate osmoregulation of the porin genes. *J Mol Biol* **222:** 567–580.

Russo, F.D., and Silhavy, T.J. (1993) The essential tension: opposed reactions in bacterial two-component regulatory systems. *Trends Microbiol* **1:** 306–310.

Sadler, J.R., and Novick, A. (1965) The properties of repressor and the kinetics of its action. *J Mol Biol* **12:** 305–327.

Savageau, M.A. (1999) Design of gene circuitry by natural selection: analysis of the lactose catabolic system in *Escherichia coli*. *Biochem Soc Trans* **27:** 264–270.

Savageau, M.A. (2001) Design principles for elementary gene circuits: elements, methods, and examples. *Chaos* **11:** 142–159.

Schwede, T., Kopp, J., Guex, N., and Peitsch, M.C. (2003) SWISS-MODEL: an automated protein homology-modeling server. *Nucleic Acids Res* **31:** 3381–3385.

Skerker, J.M., Prasol, M.S., Perchuk, B.S., Biondi, E.G., and Laub, M.T. (2005) Two-component signal transduction pathways regulating growth and cell cycle progression in a bacterium: a system-level analysis. *PloS Biol* **3:** 1770–1788.

Stephenson, K., and Hoch, J.A. (2002) Evolution of signalling in the sporulation phosphorelay. *Mol Microbiol* **46:** 297–304.

Stock, A.M., Robinson, V.L., and Goudreau, P.N. (2000) Two-component signal transduction. *Annu Rev Biochem* **69:** 183–215.

Strauch, M.A., and Hoch, J.A. (1993) Transition-state regulators – sentinels of bacillus-subtilis postexponential gene-expression. *Mol Microbiol* **7:** 337–342.

Strauch, M.A., Trach, K.A., Day, J., and Hoch, J.A. (1992) Spo0a activates and represses its own synthesis by binding at its dual promoters. *Biochimie* **74:** 619–626.

Suel, G.M., Garcia-Ojalvo, J., Liberman, L.M., and Elowitz, M.B. (2006) An excitable gene regulatory circuit induces transient cellular differentiation. *Nature* **440:** 545–550.

Tchuraev, R.N., Stupak, I.V., Tropynina, T.S., and Stupak, E.E. (2000) Epigenes: design and construction of new hereditary units. *FEBS Lett* **486:** 200–202.

Thattai, M., and van Oudenaarden, A. (2001) Intrinsic noise in gene regulatory networks. *Proc Natl Acad Sci USA* **98:** 8614–8619.

Thattai, M., and van Oudenaarden, A. (2004) Stochastic gene expression in fluctuating environments. *Genetics* **167:** 523–530.

Thomas, R., and Richelle, J. (1988) Positive feedback loops and multistationarity. *Discrete Appl Math* **19:** 381–396.

Ueki, T., and Inouye, S. (2006) A novel regulation on developmental gene expression of fruiting body formation in Myxobacteria. *Appl Microbiol Biotechnol* **72:** 21–29.

Veening, J.W., Hamoen, L.W., and Kuipers, O.P. (2005) Phosphatases modulate the bistable sporulation gene expression pattern in *Bacillus subtilis*. *Mol Microbiol* **56:** 1481–1494.

Veening, J.-W., Igoshin, O.A., Eijlander, R.T., Hamoen, L.W., Nijland, R., and Kuipers, O.P. (2008) Transient heterogeneity in extracellular protease production by *Bacillus subtilis*. *Mol Syst Biol* **4:** 184.

Wright, G.D., Holman, T.R., and Walsh, C.T. (1993) Purification and characterization of vanr and the cytosolic domain of vans – a 2-component regulatory system required for vancomycin resistance in enterococcus-faecium Bm4147. *Biochemistry* **32:** 5057–5063.

Yamamoto, K., Hirao, K., Oshima, T., Aiba, H., Utsumi, R., and Ishihama, A. (2005) Functional characterization in vitro of all two-component signal transduction systems from *Escherichia coli*. *J Biol Chem* **280:** 1448–1456.

Yoshida, T., Cai, S.J., and Inouye, M. (2002a) Interaction of EnvZ, a sensory histidine kinase, with phosphorylated OmpR, the cognate response regulator. *Mol Microbiol* **46:** 1283–1294.

Yoshida, T., Qin, L., and Inouye, M. (2002b) Formation of the stoichiometric complex of EnvZ, a histidine kinase, with its response regulator, OmpR. *Mol Microbiol* **46:** 1273–1282.

Zhu, Y., Qin, L., Yoshida, T., and Inouye, M. (2000) Phosphatase activity of histidine kinase EnvZ without kinase catalytic domain. *Proc Natl Acad Sci USA* **97:** 7808–7813.

Supplementary material

This material is available as part of the online article from:
http://www.blackwell-synergy.com/doi/abs/10.1111/j.1365-2958.2008.06221.x
(This link will take you to the article abstract).

Please note: Blackwell Publishing is not responsible for the content or functionality of any supplementary materials supplied by the authors. Any queries (other than missing material) should be directed to the corresponding author for the article.

Appendix A: Structural analysis of EnvZ–OmpR complex

Structural analysis of the SK.RR complex and consequences for model assumptions

To better understand how binding of the SK dimer and RR might happen we have complemented the analysis of the crystallized complexes with the creation and analysis of two alternative structural models for the cytoplasmic portion of the bifunctional SK EnvZ using two individually crystallized domains of the cytoplasmic portion of EnvZ (see *Experimental procedures* for details). In one of our models (Fig. A1A), which is similar to that built by Cai *et al.* (2003), the His243 of one subunit is within 10 A of the γ-phosphate of ATP in the catalytic site of the other subunit, thereby suggesting that *trans*-autophosphorylation could occur. However, for this conforma-

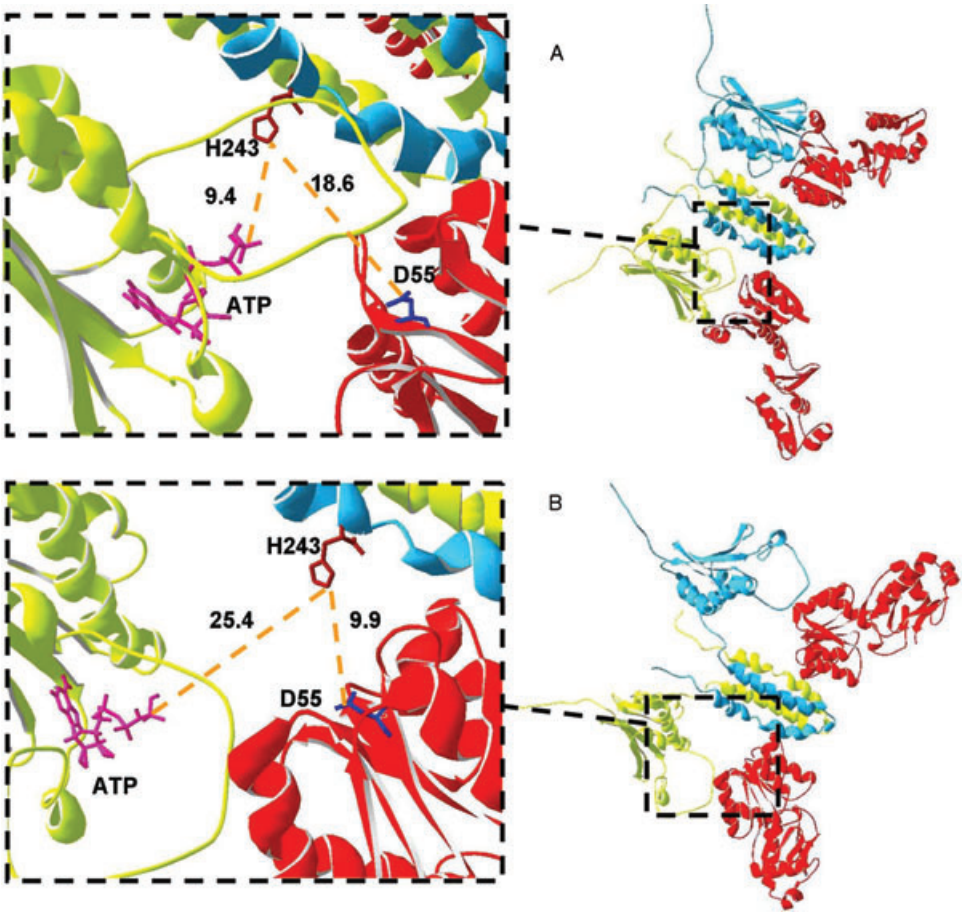

Fig. A1. Structural models for docking of the two OmpR molecules (red) onto the EnvZ dimer (the two subunits are shown in yellow and cyan). Full complexes are shown on the right; close-up views of the area around His243 (brown) for one of the EnvZ subunits are on the left. The dark blue residues in the magnification represent the Asp55 residue of OmpR. Pink residues in the magnification represent the nucleotides in the catalytic site of EnvZ.
A. Model of EnvZ based upon experimental information and created by assembling the structures in Protein Data Bank files 1JOY and 1BXD. This is similar to entry 2C2A of the Protein Data Bank, which presents the full crystal structure of a SK from the same class as EnvZ. The His243 residue is close to the nucleotide binding pocket but not to Asp55 of the RR, OmpR. The magnified section is partially rotated for better viewing.
B. A predicted model of the EnvZ structure, allowing for relaxation of the catalytic domain away from the dimerization domain. In (A) the Asp55 residue from the response regulator, OmpR, cannot access the His243 residue of the SK, whereas in (B) the response regulator prevents the His243 residue and catalytic domain of EnvZ from having access to each other.

tion of the EnvZ dimer, no productive biding can occur between EnvZ and OmpR, because His243 is buried by the catalytic domain of EnvZ and cannot come into close contact with the Asp55 of OmpR. This implies that, upon *trans*-autophosphorylation of EnvZ or upon binding of OmpR (or both), the EnvZ dimer must undergo a conformational change that allows the Asp55 of OmpR to access the His243 of one of the EnvZ monomers. The Pro295 residue, which is situated close to the loop that unites the dimerization domain of EnvZ to its catalytic domain, provides a hinge that could allow the catalytic domain to separate from the dimerization domain. By using this proline residue as a hinge, followed by loop reconstruction, we have created a new version of the EnvZ cytoplasmic domain in which the catalytic domain relaxes away from its dimerization domain that contains His243 (Fig. A1B). With this conformational shift the Asp55 and His243 become accessible but the distance from His243 to the catalytic site is too large for autophosphorylation to occur. The methods used to obtain the two structures do not pinpoint the precise mechanism of the conformational change. However, we view the resulting structures as an indication that some conformational change is required between the cyclic autophosphorylation and phosphotransfer reactions. This suggestion is supported by the analysis of the crystallized complexes, in which the catalytic ATP binding domain of the SKs are distant from the catalytic His residue. Independent of the actual conformational change and how it happens, the binding of OmpR is likely to disturb the access of the ATP binding domain to His243, thus preventing autophosphorylation. Taken together, the previous arguments do not support the possibility of autophosphorylation of the SK while in the SK.RR complex.

Appendix B: analysis of transient responses

Response to gradually varying changes

One can argue that the bistable design may respond slower to gradual changes of the input signal because the full-scale response commences only after the signal exceeds a given switching threshold. Therefore, we investigated how the designs with alternative dynamic characteristics respond to gradually varying changes in the autophosphorylation rate. First, we investigated how the graded and hysteretic designs of TCS respond to a linear increase of the phosphorylation rate followed by a linear decrease in that same rate (Fig. A2). The magnitude of the response (maximal concentration of RR~P) depends on the maximal amplitude of the signal and on the duration of the signal. The analysis presented in Fig A2B and C confirms the results obtained with an instantaneous change in input signal; namely, that the bistable design responds faster unless the input signal amplitude is close to the switching threshold. Similar conclusions are reached when one analyses the frequency response of the system to a periodic (sinusoidal) signal $k_{ap} = k^0_{ap}(0.5001 + 0.5\sin[\omega t])$. For low frequencies, the concentration of RR~P tracks the input signal, reaching values close to the steady-state response at k^0_{ap} when the input signal reaches its peak. With increasing frequency the system does not have time for a full-scale response and the amplitude of the RR~P oscillations is attenuated. We computed the cut-off frequency – the value of ω at which the amplitude of the RR~P oscillation is 50% of the maximum obtained at low frequency (Fig. A3). The results are shown in Figs A2 and A3 and indicate that, even for gradual changes in the strength of the input signal, the bistable design is faster except when close to or within the borders of the bistability region.

Controlled comparisons of the transient responses for alternative designs

An analysis of the results presented in Figs 4A, B, A2 and A3 reveals significant differences between response times of bistable and monostable designs. However, it is not clear which design features are responsible for these differences. They might result from the presence of an alternative phosphatase, the presence of bistability, differences in the steepness of the signal–response curve, differences in the value of input signal at which the response saturates, or some combination of these features. To differentiate among these four possibilities, transient times for the ON and OFF responses were calculated for four distinct implementations of the two different designs for the TCS network. These implementations were chosen so as to control for each of the design aspects described above (Fig. S3):

Implementation I. A monostable design with a bifunctional SK (the same as Fig. 2A, solid line)
Implementation II. A bistable design with a monofunctional SK (the same as Fig. 2A, dashed line)
In this implementation, the RR is dephosphorylated by an alternative phosphatase, Ph. The concentrations and kinetic parameters of this phosphatase are chosen to match those of the SK in Implementation I. As a result, the region of bistability is symmetrically disposed about a value of the input signal corresponding to 50% of its saturating value in Implementation I.
Implementation III. A variation of Implementation I with a sharper response to the input signal
This variation is achieved by reducing the rate constant for the phosphatase reaction so that a 95% saturation of the bifunctional system occurs when the input signal has a value that lies in the middle of the bistability range for Implementation II.
Implementation IV. A variation of Implementation II that lacks bistability
In this implementation, the rate constant for dissociation of the dead-end complex is increased by 10-fold so that no bistability is observed. For this design we also increased the phosphatase activity twofold in order to maintain a 50% saturation for values of the input signal that lies in the middle of the bistability range for Implementation I.

The temporal responsiveness of the alternative designs is depicted in Fig. S3B and C. Fig. S3B allows comparison of the transient OFF-to-ON times for these designs. Systems are initially in the OFF steady state corresponding to $k_{app} = 0.0001$. We instantaneously change k_{app} to a new higher value (*x*-axis) and compute the time it takes the system to reach 90% of the new steady state. Comparing the response times between Implementation I and Implementation III suggests that an increase in the steepness of the signal–response curve results in a slower response. The monostable, monofunctional design (Implementation IV) is faster than both implementations of the bifunctional design

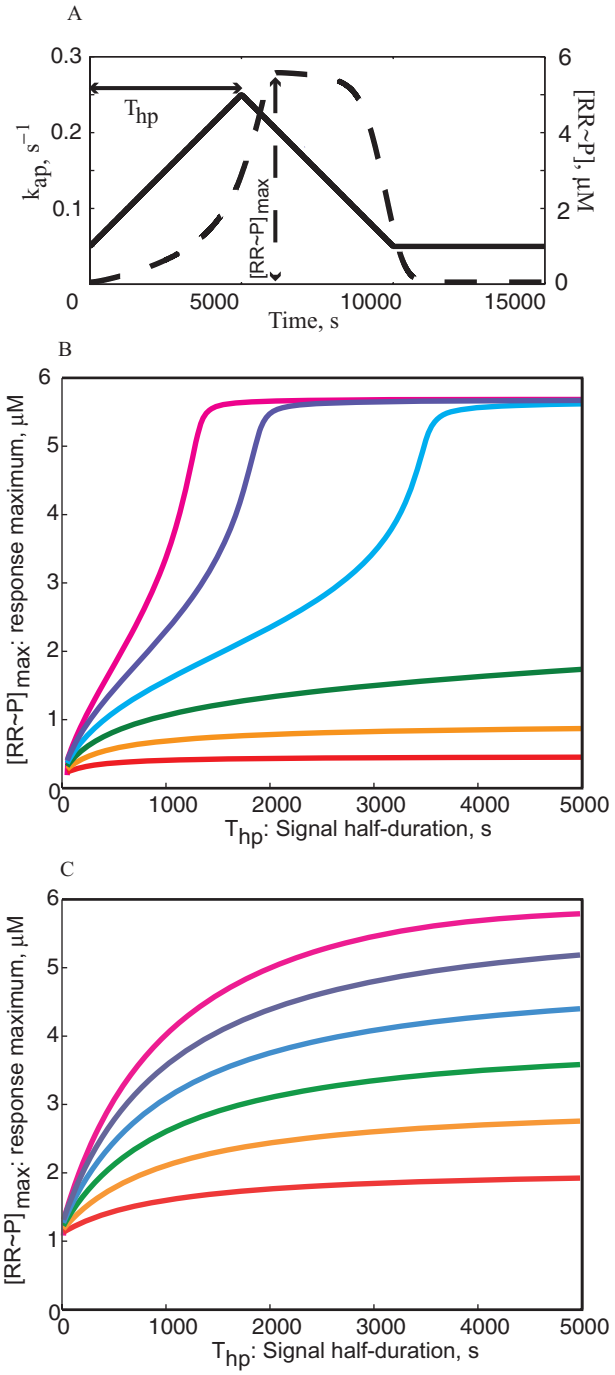

Fig. A2. Transient responses to a triangular pulse of input signal by the bistable and monostable designs.
A. Sample pulse of the autophosphorylation rate (right axis, solid line) and the corresponding response of the bistable design (left axis, dashed line). T_{hp} – the half-duration of the pulse and $[RR\sim P]_{max}$ – the maximum concentration of RR~P in the response are indicated.
(B) and (C) show how the maximum concentration in the response varies with pulse duration (i.e. $[RR\sim P]_{max}$ versus T_{hp}) for various amplitudes of the input signal. The systems are initially at equilibrium with $k_{ap} = 0.05\ s^{-1}$, and at $t = 0$ they are subjected to a triangular pulse of the input signal as shown in (a) with various maximum amplitudes: $k_{ap} = 0.10\ s^{-1}$ (red), $k_{ap} = 0.15\ s^{-1}$ (orange), $k_{ap} = 0.20\ s^{-1}$ (green), $k_{ap} = 0.25\ s^{-1}$ (blue), $k_{ap} = 0.30\ s^{-1}$ (purple) and $k_{ap} = 0.35\ s^{-1}$ (magenta).
B. Temporal response of the bistable design.
C. Temporal response of the monostable design.
Note that the curves in (B) and (C) are very similar to those shown in Fig. 4A and B, indicating that the bistable design is faster unless the amplitude of the input signal is close to the switching threshold.

(Implementations I and III), suggesting that the differences in response time between the different designs are associated with the presence of an alternative phosphatase rather than with bistability *per se*. On the other hand, a discontinuous slow-down in the response times for Implementation II immediately above the switching threshold is associated with a discontinuity in the steady-state response. Similar conclusions are obtained from the analysis of the transient ON-to-OFF times for these designs (Fig. S3C). In this case, the systems are initially in the ON steady state corresponding to $k_{app} = 0.5$; we instantaneously change k_{app} to a new lower value (*x*-axis), and then compute the time it takes the system to reach 90% of the new steady state.

Our analysis of the transient responses (Figs 3, A2 and A3) for the two alternative TCS designs indicates that (i) the monostable design is slower than the bistable design away from the discontinuous switching thresholds and that (ii) the bistable design is much slower than the monostable design near the switching threshold. We asked whether this pattern of transient response is intrinsic to bistability *per se* or whether other differences between the designs (such as the presence of an alternative phosphatase, differences in steepness of the signal–response curve or differences in values at which the signals saturate) might be responsible. Analysis of the different designs indicates that:

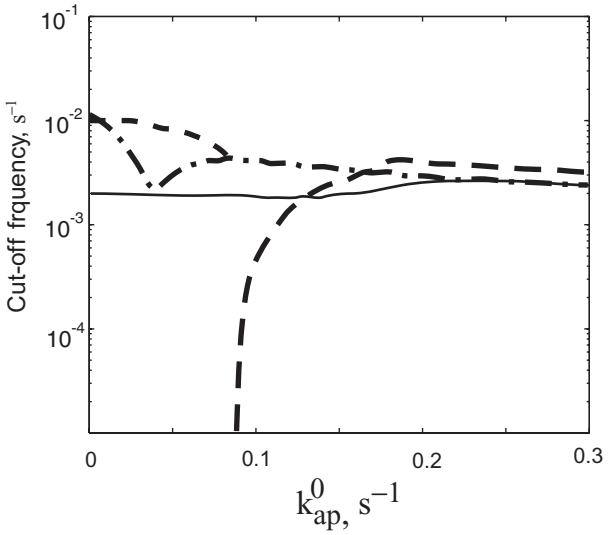

Fig. A3. Comparison of the frequency response for the different designs. The simulations are done as follows. An input signal of the form $k_{ap} = k^0_{ap}(0.5001 + 0.5\sin[\omega t])$ is applied to the system for a period long enough to establish a steady-state oscillation. For each amplitude of the input signal k^0_{ap}, we calculate the cut-off frequency, ω, at which the amplitude of the RR~P response is half of its maximum amplitude at lowest frequency. Line designations are the same as Fig. 2A.

i The faster response of the bistable design is associated with the presence of an alternative phosphatase. This is supported by the fact that the monofunctional, monostable design (with an alternative phosphatase) is also faster than the bifunctional, monostable design (without an alternative phosphatase).

ii The slower response of the bistable design near the switching region is associated with the discontinuity of the signal–response curve. This is supported by the fact that the monofunctional, monostable design is always faster than the bifunctional monostable design.

